Published in final edited form as:
Protein Expr Purif. 2008 March ; 58(1): 32–41.

Baculovirus-mediated expression, purification, and characterization of a fully activated catalytic kinase domain construct of the 70 kDa 40S ribosomal protein S6 kinase-1 αII isoform (S6K1αII)

Malik M. Keshwani[a], **Duncan B. Ross**[b], **Timothy J. Ragan**[b], and **Thomas K. Harris**[b,*]

a*Department of Chemistry, University of Miami, P. O. Box 249118, Coral Gables, FL 33124-0431*

b*Department of Biochemistry and Molecular Biology, University of Miami Miller School of Medicine, P. O. Box 016129, Miami, FL 33101-6129*

Abstract

S6K1αII is a member of the AGC subfamily of serine-threonine protein kinases, whereby catalytic activation requires dual phosphorylation of critical residues in the conserved T-loop (T229) and hydrophobic motif (HM; T389) regions of its catalytic kinase domain [S6K1αII(ΔAID); deletion of C-terminal autoinhibitory domain residues 399-502]. With regard to mimicking the synergistic effect of full dual site phosphorylation, baculovirus-mediated expression and affinity purification of the His_6-S6K1αII(ΔAID)-T229E,T389E double mutant from Sf9 insect cells yielded enzyme with

*To whom correspondence should be addressed: T.K.H.: Tel: 305-243-3358; Fax: 305-243-3955; and E-mail: tkharris@miami.edu

[1]*Abbreviations used*:

AID
C-terminal autoinhibitory domain of S6K1

ATP
adenosine 5′-triphosphate

His_6-PDK1(ΔPH)
N-terminal His_6 affinity tagged recombinant catalytic domain of PDK1 (residues 51-359)

His_6-S6K1αII(ΔAID)-T389E
N-terminal His_6 affinity tagged recombinant catalytic domain of the αII isoform of S6K1 (residues 1-398) and including the T389E mutation

HM
hydrophobic motif

PDK1
phosphoinositide-dependent protein kinase-1

PH
C-terminal pleckstrin homology domain of PDK1

PIF
PDK1-interacting fragment

S6K1
70 kDa 40S ribosomal protein S6 kinase-1

compromised activity. Higher activity preparations were generated using the Sf9 purified His_6-S6K1αII(ΔAID)-T389E single mutant isoform, which was in vitro phosphorylated by the upstream T229 kinase, PDK1 (~75 nmol/min/mg). Most significantly, we report that the His_6-S6K1αII (ΔAID)-T389E construct was generated in its most highly active form (250 nmol/min/mg) by baculovirus-mediated expression and purification from Sf9 insect cells that were *coinfected* with recombinant baculovirus expressing the catalytic kinase domain of PDK1 [His_6-PDK1(ΔPH)]. Approximately equal amounts of fully activated His_6-S6K1αII(ΔAID)-T389E (5 ± 1 mg) and His_6-PDK1(ΔPH) (8 ± 2 mg) were His_6 affinity co-purified 60 h after initial coinfection of 200 mL of Sf9 insect cells (2×10^6 cells/mL), which were resolved by MonoQ anion exchange chromatography. ESI-TOF mass spectrometry, MonoQ anion exchange chromatography, and kinetic assays showed His_6-PDK1(ΔPH) to phosphorylate T229 to ~100% after co-expression in Sf9 insect cells as compared to ~50% under in vitro conditions, raising interest to mechanistic components not fully achieved in the in vitro reaction. Generation of fully activated S6K1 will facilitate more rigorous analysis of its structure and mechanism.

Keywords

S6K1-T389E; phosphoinositide-dependent protein kinase-1; PDK1; Sf9 insect cells; baculoviral coinfection; ESI-TOF; MonoQ anion exchange; protein phosphorylation

Introduction

A key requirement for higher eukaryotic cells in sustaining prolific capacity is growth regulation, whereby increasing cellular mass and size prerequisite to division derives from coordinate macromolecular biosynthesis. The 70-kDa 40S ribosomal protein S6 kinase-1 (S6K1) is a key enzyme in coordinating cell growth with proliferation, as *mitogen*, *nutrient*, and *energy status* signaling pathways converge to activate S6K1 and initiate protein translation [1-5]. Two S6K1 isoforms (Accession No. **NM003161**; αI and αII isoforms) are produced from a single gene by alternative mRNA splicing and the use of an alternative translational start site [6]. The 525 residue αI isoform contains an N-terminal 23 residue segment that encodes a polybasic nuclear localization motif; whereas the cytoplasmic αII isoform starts at a Met residue equivalent to Met24 in the αI isoform; and the sequences of both isoforms are identical thereafter (Fig. 1A).

S6K1 is a member of the AGC subfamily of serine-threonine protein kinases in which amino acid sequences are conserved in a segment of the catalytic kinase domain known as the activation loop or T-loop, as well as in a segment near the C-terminus of the kinase domain known as the hydrophobic motif (HM) [7]. Similar to other AGC kinase family members, catalytic activation of S6K1 minimally requires dual phosphorylation of a critical residue in both the T-loop and HM. For the full length S6K1αI isoform these residues correspond to T252 and T412, respectively [8]; whereas in the S6K1αII isoform the identical residues correspond to T229 and T389 (Fig. 1A) [9]. With combined knowledge from available amino acid sequence alignments and X-ray structures, molecular modeling and biochemical testing now provide strong evidence for a common AGC kinase activation mechanism in which the C-terminal phosphorylated hydrophobic motif interacts with a phosphate binding pocket located in the small N-lobe of the kinase [10]. This intramolecular interaction acts synergistically with T-loop phosphorylation to stabilize the active conformation, whereby a critical Glu residue in the αC-helix forms an ion pair with the catalytic Lys that functions to position the terminal phosphate of ATP for phosphotransfer in the kinase reaction.

In recognizing the synergistic role of AGC kinase dual site phosphorylation, neither an X-ray three dimensional structure nor a kinetic mechanism has been reported for any S6K1 isoform

or domain construct. This derives largely from the inability to generate fully T229 phosphorylated and activated S6K1. Previous studies reported high yield baculovirus-mediated expression and purification from Sf21 insect cells of N-terminal His_6 affinity tagged catalytic kinase domain constructs of S6K1αI in both its native and T412E mutant forms [11,12], which we will refer to as His_6-S6K1αI(ΔAID) and His_6-S6K1αI(ΔAID)-T412E. Similarly, Flag-S6K1αI(ΔAID) and Flag-S6K1αI(ΔAID)-T412E constructs were readily obtained from HEK293 cells [12]. In all cases, Western analysis showed little or no T-loop (T252 in αI) phosphorylation. The highest degree of catalytic activation (40-50 nmol/min/mg) was obtained by incubation of the T412E mutant with the T-loop upstream kinase, PDK1, which resulted in ~60% T252 phosphorylation [11,12]. Similarly, T229 of the GST-S6K1αII-T389E isoform was unphosphorylated when purified after baculovirus-mediated expression in Sf9 insect cells [13]. Surprisingly, Flag-S6K1αII(ΔAID)-T389E purified from HEK293 cells showed some degree of T-loop phosphorylation and catalytic activation, but neither was analytically quantified [13]. Such ongoing efforts have been motivated by the observation that overexpression and affinity purification of S6K1 catalytic domain constructs containing phosphomimicking mutations of both the critical T-loop and HM residues yielded enzyme with less activity than the partially T229 phosphorylated form (unpublished results).

In this paper, we demonstrate by (i) Western analysis, (ii) ESI-TOF, (iii) MonoQ anion exchange chromatography, and (iv) kinetic assays that the N-terminal His_6 affinity tagged catalytic kinase domain construct of the αII isoform of S6K1 [Fig. 1B; His_6-S6K1αII(ΔAID)-T389E, residues 1-398] can be generated in its most highly active form (250 nmol/min/mg) by baculovirus-mediated expression and purification from Sf9 insect cells that are coinfected with recombinant PDK1. In addition, we show that His_6-S6K1αII(ΔAID)-T389E is purified from Sf9 cells solely infected as a largely homogeneous species that does not contain any post-translational modifications. The preparation and characterization of His_6-S6K1αII(ΔAID)-T389E in both its T229 phosphorylated and unphosphorylated forms will facilitate more detailed structural and kinetic studies on its mechanisms of action and regulation.

Materials and methods

Materials

The Bac-to-Bac® Baculovirus Expression System, and Nitrocellulose Membrane Filter Paper Sandwich were from Invitrogen, Inc. (Carlsbad, CA). The ÄKTAbasic 100 (FPLC), Prepacked HisTrap HP column (5 mL), and Tricorn™ Mono Q™ 5/50 GL anion exchange column were from GE Healthcare Biosciences (Piscataway, NJ). The cOmplete™ Protease Inhibitor Cocktail Tablets were from Roche Applied Science (Indianapolis, IN). Phospho-S6K1 (Thr229) polyclonal antibody was from Novus Biologicals (Littleton, CO). S6K/RSK2 Substrate Peptide 1 (S6K1-Tide, RRRLSSLRA) was from Upstate USA, Inc. (Charlottesville, VA). Amicon® Ultra Centrifugal Filter Device concentrators were from Millipore (Billerica, MA). All other chemicals, salts, and buffers were from Sigma, Inc. (St. Louis, MO).

Baculovirus-mediated (co-)expression and affinity purification of His_6-S6K1αII(ΔAID)-T389E

The pFastbac™1 vector containing either the His_6-S6K1αII(ΔAID)-T389E or His_6-PDK1(ΔPH) recombinant fusion constructs (Supplementary Material) was used to generate their respective recombinant baculovirus using the Bac-to-Bac® Baculovirus Expression System. Recombinant P2 viral stocks of His_6-S6K1αII(ΔAID)-T389E was used to infect 200 mL spinner flask cultures of Sf9 cells in the mid-logarithmic phase of growth (2×10^6 cells/mL) so that a multiplicity of infection (MOI) of 2 viral particles/cell was obtained. For coinfection with both His_6-S6K1αII(ΔAID)-T389E and His_6-PDK1(ΔPH), a MOI = 1 was used for each recombinant baculoviral construct. In every case, the infected cells were incubated at 27 °C for 56-60 h and harvested by centrifugation for 10 min at 4 °C at 3000 rpm in a Beckman

tabletop centrifuge. The cells were re-suspended in 50 mL of buffer (50 mM Tris-HCl, pH 7.5, 300 mM NaCl, 50 mM imidazole, 1 mM 2-mercaptoethanol, 1 mM benzamidine, 0.2 mM PMSF, and cOmplete™ Protease Inhibitor Cocktail), and were immediately stored at -80 °C. The re-suspended frozen cells were allowed to thaw on ice for 15 min before addition of 2 μL of benzonase and 1 mM $MgCl_2$. Then, the cells were allowed to continue thawing for 1 h, which resulted in efficient cell lysis and oligonucleotide degradation. Cell debris was pelleted by centrifugation for 45 min at 4 °C at 14,000 rpm in a SS34 rotor.

The soluble lysate, containing either His_6-S6K1αII(ΔAID)-T389E alone or both His_6-S6K1αII(ΔAID)-T389E and His_6-PDK1(ΔPH), was directly loaded by FPLC (1 mL/min) onto a 5 mL size Ni^{2+} Sepharose HiTrap HP affinity column equilibrated at 4 °C in 50 mM Tris-HCl, pH 7.5, 300 mM NaCl, 50 mM imidazole, 1 mM 2-mercaptoethanol, and 5% (v/v) glycerol. The column was subsequently washed until the absorbance at 280 nm returned to baseline, and the recombinant His_6 affinity tagged enzyme(s) was eluted by linear increasing of the imidazole concentration from 50 to 500 mM at 1 mL/min for 30 min. Chromatographic fractions (1 mL) containing His_6 affinity tagged enzyme were detected by absorbance at 280 nm and confirmed by SDS-PAGE. For preparations involving coinfection of Sf9 insect cells with both His_6-S6K1αII(ΔAID)-T389E and His_6-PDK1(ΔPH), chromatographic fractions containing both enzymes were combined, diluted 10-fold in 50 mM Tris-HCl, and loaded by FPLC (1 mL/min) onto a MonoQ anion exchange column, which was equilibrated at 4 °C in 20 mM Tris-HCl, pH 7.3, with 20 mM NaCl. The column was subsequently washed until the absorbance at 280 nm returned to baseline, which indicated that all His_6-PDK1(ΔPH) had passed through the column. His_6-S6K1αII(ΔAID)-T389E was eluted by linear increasing of the NaCl concentration from 20 to 1000 mM at 0.5 mL/min for 40 min. All purified enzymes were concentrated and exchanged into storage buffer (50 mM Tris-HCl, pH 7.5, 270 mM sucrose, 150 mM NaCl, 0.1 mM EGTA, 0.2 mM PMSF, 1 mM benzamidine, 0.1% 2-mercaptoethanol, and 0.03% Brij 35) using Amicon® Ultra Centrifugal Filter Devices. Each purified enzyme (~25 μM) stored as 0.1-1 mL aliquots at -80 °C. Protein concentrations were determined using the Bio-Rad Protein Assay Kit with bovine serum albumin as a standard.

In vitro activation of His_6-S6K1αII(ΔAID)-T389E by PDK1

His_6-S6K1αII(ΔAID)-T389E purified from Sf9 cells solely infected was reacted with active His_6-PDK1(ΔPH) purified from Sf9 cells coinfected with His_6-S6K1αII(ΔAID)-T389E. The phosphorylation reaction was performed at 25 °C in kinase reaction buffer consisting of 50 mM Tris-HCl buffer, pH 7.5, 0.1% 2-mercaptoethanol, 10 mM $MgCl_2$, 2 μM okadaic acid, 1mM EDTA, 1 mM EGTA, and 100 μM of either cold or [γ-^{32}P]ATP (~500-1000 cpm/pmol). For determination of the time dependence and mole fraction of T229 phosphorylation of His_6-S6K1αII(ΔAID)-T389E (either 2 or 15 μM) by His_6-PDK1(ΔPH) (10 nM), 30-μL aliquots were removed from a 500-μL reaction mixture at different times (0, 30, 60, 90, 120, 180, 300, 600, 900, 1200, and 1800 s) and quenched with 30 μL of 75 mM phosphoric acid. Then, the quenched reaction was applied as 30 μL aliquots to two different pieces of P81 phosphocellulose paper for quantification of micromolar amounts of ^{32}P-radiolabeled protein, as described below for steady-state kinetic assays. Control assays were carried out in parallel in which either the His_6-PDK1(ΔPH) enzyme or the His_6-S6K1αII(ΔAID)-T389E substrate were omitted; and in each case no ^{32}P-radiolabled protein could be detected above the background amounts of radiation obtained in the absence of both constructs (≤250 cpm).

To determine site-specific phosphorylation, a 100 μL reaction containing 10 nM His_6-PDK1(ΔPH) (2.5 pmol) and 2 μM His_6-S6K1αII(ΔAID)-T389E (200 pmol) was allowed to proceed at 30 °C for 30 min; and this reaction mixture was used for trypsin digestion and HPLC resolution of ^{32}P-radiolabeled peptides. First, cysteine residues were reduced by addition of 0.5 mL of 50 mM Tris-HCl, pH 7.5, containing 50 mM 2-mercaptoethanol. Free cysteines were

protected from re-oxidation by subsequent addition of 50 μL of 500 mM iodoacetamide incubation in the dark at room temperature for 20 min. Excess unreacted iodoacetamide was depleted from the reaction mixture by further addition of 30 μL of 500 mM 2-mercaptoethanol and incubation at room temperature for 5 min. Proteolytic digestion was carried out by addition of 1 μg trypsin and incubation at 37 °C for 5 h, followed by subsequent addition of 1 μg trypsin and incubation at 37 °C overnight. The individual reaction mixtures (~200 μL) were diluted to 1 mL with solvent A [0.1% (v/v) trifluoroacetic acid in water]. The 1 mL samples were directly loaded by HPLC (0.5 mL/min) onto a μRPC C2/C18 column (Amersham) equilibrated in 100% solvent A. The column was subsequently washed in this buffer for 5 min, and the peptides were eluted by linear increasing solvent B [80% acetonitrile and 0.07% (v/v) trifluoroacetic acid in water] from 0% to 50% in 1 h at a flow rate of 0.4 mL/min, while 300 μL were collected for each fraction. ^{32}P-radiolabeled peptides were detected by scintillation counting of 30 μL of each chromatographic fraction.

SDS-PAGE and Western analysis

Protein samples in SDS sample buffer were heated at 95 °C for 5 min and cooled on ice. All analytical SDS-PAGE were performed on 4-12% gradient Bis-Tris polyacrylamide gels (NuPage), which were developed at 30 mA (constant) for ~2 h or until the tracking dye reached the bottom of the slab. For Western analysis of His_6-S6K1αII(ΔAID)-T389E, proteins were transferred from the gel to Nitrocellulose Membrane Filter Paper Sandwich (Invitrogen) in a semidry blotting apparatus using Towbin buffer (25 mM Tris base, pH 8.3, 0.19 M glycine, and 20% ethanol) as transferring solution. The resulting membranes were probed with the phospho-S6K1 (Thr229) polyclonal rabbit antibody according to the manufacturer's instructions (Novus Biologicals). Detection of immuno-protein complexes was carried out using secondary anti-rabbit antibody conjugated to horseradish peroxidase (HRP) (Cell Signaling Technology, Inc.) and Super Signal West Pico Luminal/Enhancer Solution and peroxide (Pierce).

ESI-TOF mass spectrometry analysis

Electrospray ionization-time of flight mass spectrometry (ESI-TOF) was performed at Johns Hopkins University Mass Spectrometry/Proteomics Facility (Baltimore, MD), using nano-flow HPLC (Eksigent nano-2DLC pump) connected to an Applied Biosystems QSTAR QTOF. The QSTAR is an electrospray ionization mass spectrometer with a TOF analyzer and can detect masses up to 12,000 Da for singly charged species. First, the protein samples were trapped on a column made with 2 cm of a 10-15 μm polymeric reversed phase material packed into 75 μm fused silica. The column was 8 cm of the same polymeric material with 5 μm particle size bomb packed in 75 μm fused silica. Sample was loaded onto the trap at 5 μL/min in 95% Buffer A (0.1% formic acid) and 5% Buffer B (0.1% formic acid and 90% acetonitrile). The trap was switched into the nanoflow side (300 nL/min), where a gradient starting at 15% Buffer B was run to 50% B in 35 min, then run to 75% B in 45 min, then bumped to 100% B and back to initial conditions. A spray voltage of 2.2 kV was used for the QSTAR spectrometer, and only MS was used to get multiply charged envelopes belonging to intact protein. Calibration was performed using a mixture of CsI (MW 132.9049), verapamil (MW 455.2904), and synthetic peptide ALILTLVS (MW 829.5393). Deconvolution of charged states was analyzed using the Biotools software (Applied Biosystems) and a Bayesian protein reconstruction mass range of 600-1800 Da with 15 iterations.

MonoQ anion exchange chromatography

Preparations of His_6-S6K1αII(ΔAID)-T389E enzyme (~1 mg) were diluted into 20 mM Tris-HCl and 20 mM NaCl buffer, pH 7.3, and loaded by FPLC (1 mL/min) onto a Tricorn Mono Q™ 5/50 GL ion exchange column, which was equilibrated at 4 °C in the same buffer. The

column was subsequently washed until the absorbance at 280 nm returned to baseline. Differentially phosphorylated isoforms of His_6-S6K1αII(ΔAID)-T389E were eluted by linear increasing of the NaCl concentration from 20 to 1000 mM at 0.5 mL/min for 40 min; and fractions were analyzed for S6K1 activity as described below.

Steady-state kinetic assays

Enzyme activities were determined by measuring initial velocities for His_6-S6K1αII(ΔAID)-T389E catalyzed phosphorylation of a commercially available S6K/RSK model peptide substrate 1 (S6K1-Tide, RRRLSSLRA). The residue of the peptide substrate that undergoes phosphorylation is underlined. The 100-μL model peptide phosphorylation reactions were performed at 30 °C in kinase reaction buffer consisting of 40 mM MOPS buffer, pH 7.0, 0.1% 2-mercaptoethanol, 10 mM $MgCl_2$, and 1 mM EDTA. Initial velocities (μM s^{-1}) were measured (i) using 50 μM [γ-^{32}P]ATP (~500-1000 cpm/pmol) for varying S6K1-Tide concentrations (0.5, 1, 2, 3, 5, 10, 15, 30, and 50 μM) and (ii) using 50 μM S6K1-Tide for varying [γ-^{32}P]ATP concentrations (0.5, 1, 2, 3, 5, 10, 15, 30, and 50 μM). The assays were initiated by addition of 20 nM kinase.

For all kinase assays, 20-μL aliquots were removed at three different times (ranging from 5 to 15 min), mixed with 20-μL of 75 mM phosphoric acid, and applied to P81 phosphocellulose paper (2 × 2 cm). After 30 s, the papers were washed (3×) in 1 L of fresh 75 mM phosphoric acid for 10 min, then rinsed with 50 mL of acetone, and placed in the hood (≤5 min) to dry. The specific radioactivity of ^{32}P-radiolabeled S6K1-Tide (SA^{Tide}, cpm/pmol) was determined from radioactivity detected by scintillation counting of the known amount of total S6K1-Tide that was applied to the P81 paper; and the micromolar amount of phosphorylated S6K1-Tide product formed at each time point was determined by reference to the specific radioactivity of [γ-^{32}P]ATP (SA^{ATP}, ~500-1000 cpm/pmol) and the volume of the aliquot removed for quenching (20 μL). Initial velocities (ν, μM s^{-1}) were measured under conditions where total product formation represented ≤10% of the initial substrate concentration. Control assays were carried out in parallel in which either the enzyme or the peptide substrate were omitted; these values were always ≤5% of the activity measured in the presence of these reagents. To better facilitate kinetic comparisons between S6K1 constructs of different molecular weight, initial velocities were normalized to enzyme concentration to yield apparent first-order rate constants, k (s^{-1}) = ν/[E_{tot}]. Otherwise reported, one unit of activity was defined as the amount of enzyme required to catalyze phophorylation of one nmol peptide substrate in 1 min.

Results and discussion

Expression, purification, and activation of His_6-S6K1αII(ΔAID)-T389E by PDK1

The human lung Marathon-Ready cDNA library (Clontech) served as a convenient template for efficient generation of cDNA coding for the catalytic domain of the S6K1αII protein kinase [S6K1αII(ΔAID); residues 1-398] (Fig. 1A). PCR was further used to extend this cDNA to code for an N-terminal His_6 affinity tag and a PreScission Protease recognition sequence (Fig. 1B), which was subcloned into the pFastbac™1 vector. The His_6-S6K1αII(ΔAID) construct was mutated to yield the His_6-S6K1αII(ΔAID)-T389E construct for generation of recombinant baculovirus using the Bac-to-Bac Baculovirus Expression System (Invitrogen). Using MOI = 2 and a time of harvest 56-60 h after post infection, His_6-S6K1αII(ΔAID)-T389E was overexpressed and His_6 affinity purified, typically yielding 15 ± 2 mg from initial infection of 4×10^8 total insect cells (Table 1). Fig. 2A shows that His_6-S6K1αII(ΔAID)-T389E was efficiently purified to ≥95% homogeneity (lane 3), as judged by Coomassie blue staining of 4-12% SDS-PAGE. His_6-S6K1αII(ΔAID)-T389E purified from Sf9 cells solely infected was largely inactive (2 ± 1 nmol/min/mg), and no T229 phosphorylation was detected by Western analysis (Fig. 2C, lane 1). Incidentally, minor amounts of high molecular weight protein

impurities were observed with His_6 affinity purified His_6-S6K1αII(ΔAID)-T389E, which could be easily removed by heparin sepharose chromatography.

In order to generate fully T229 phosphorylated, active His_6-S6K1αII(ΔAID)-T389E enzyme, the Sf9 insect cells were co-transfected with recombinant baculovirus expressing His_6-S6K1αII(ΔAID)-T389E along with recombinant baculovirus expressing the catalytic domain construct of the T229 upstream kinase, PDK1 [His_6-PDK1(ΔPH); residues 51-359]. Using an MOI = 1 for each construct and a time of harvest 56-60 h after post infection, His_6-S6K1αII (ΔAID)-T389E and His_6-PDK1(ΔPH) were co-expressed and purified, typically yielding 5 ± 1 mg and 8 ± 2 mg, respectively, from initial infection of 4×10^8 total insect cells (Table 2). Fig. 2B shows that after initial His_6 affinity purification, about equal amounts of both His_6-S6K1αII(ΔAID)-T389E (M_r = 50 kDa) and His_6-PDK1(ΔPH) (M_r = 37 kDa) were co-expressed and co-purified (lane 3). The two enzymes were further resolved to ≥95% homogeneity by MonoQ anion exchange chromatography, whereby (i) flow through fractions of His_6-PDK1(ΔPH) were concentrated and stored (lane 4) and (ii) His_6-S6K1αII(ΔAID)-T389E eluted near 0.46 M NaCl (lane 5). In this case, purified His_6-S6K1αII(ΔAID)-T389E showed very high activity to the S6K1-Tide substrate (250 ± 10 nmol/min/mg); and Western blotting with the phospho-S6K1 (T229) antibody revealed approximately equal amounts of two distinct S6K1 species with significant T229 phosphorylation (Fig. 2C, lane 2). As determined in the ESI-TOF studies described below, the slower mobility protein species is due to T229 phosphorylated His_6-S6K1αII(ΔAID)-T389E containing one additional site of phosphorylation. Finally, Western blotting with the phospho-PDK1 (S241) antibody showed that His_6-PDK1(ΔPH) was purified in its S241 phosphorylated and active form (Fig. 2B, lane 4), as required for its ability to activate S6K1 during co-expression.

In order to test the ability of purified active His_6-PDK1(ΔPH) to activate His_6-S6K1αII(ΔAID)-T389E under in vitro conditions, 1 μM of unphosphorylated inactive His_6-S6K1αII(ΔAID)-T389E purified from cells solely infected (Fig. 2A, lane 3) was pre-incubated for 30 min at 25 °C with an equivalent amount of purified active His_6-PDK1(ΔPH). Afterwards, His_6-S6K1αII(ΔAID)-T389E showed increased activity (75 ± 10 nmol/min/mg), and Western analysis confirmed a significant amount of T229 phosphorylation (Fig. 2C, lane 3). In this case, a much smaller but consistently detectable amount of the slower mobility T229 phosphorylated His_6-S6K1αII(ΔAID)-T389E species appeared, which ESI-TOF revealed to be due to one additional site of phosphorylation (see below).

By utilizing radiolabeled [γ-^{32}P]ATP, the time dependence and mole fraction of T229 phosphorylation was determined using 10 nM His_6-PDK1(ΔPH) (enzyme) and either 2 μM or 15 μM of His_6-S6K1αII(ΔAID)-T389E (substrate) (Fig. 2D); and the specificity of protein phosphorylation was analyzed by ^{32}P-phosphopeptide mapping (Fig. 2E). As previously reported for PDK1-catalyzed T-loop phopshorylation of the His_6-S6K1(ΔAID)-T412E αI isoform [8], a limiting sub-stoichiometric amount (~50%) of site-specific T229 phosphorylation was achieved after 30 min for both 2 μM and 15 μM amounts of His_6-S6K1αII(ΔAID)-T389E (substrate). In both cases, no amount of His_6-S6K1αII(ΔAID)-T389E-catalyzed autophosphorylation of any residue was detected in control reactions. More interestingly, a significant “lag” in the reaction progress curve was observed at the higher S6K1 concentration, indicating hysteretic or kinetic complexity deriving from additional “states” being present in either the PDK1 or S6K1 macromolecules [14]. In both cases, His_6-S6K1αII(ΔAID)-T389E treated with 10 nM PDK1 was activated to the same extent as when 1 μM PDK1 was used (75 ± 10 nmol/min/mg). Thus, it remains unclear as to why in vitro PDK1-catalyzed T229 phosphorylation of His_6-S6K1αI(ΔAID)-T412E is sub-stoichiometric.

ESI-TOF and MonoQ analysis of His_6-S6K1αII(ΔAID)-T389E activation by PDK1

To further examine the molecular basis by which S6K1 activity is generated, ESI-TOF and MonoQ anion exchange chromatography were carried out on His_6-S6K1αII(ΔAID)-T389E (i) purified from cells solely infected both before and after 30 min in vitro treatment with His_6-PDK1(ΔPH) and (ii) His_6-S6K1αII(ΔAID)-T389E purified from cells coinfected with His_6-PDK1(ΔPH). Electrospray on an intact protein determines the mass by multiply charging the molecule such that a charge envelope is seen in the spectrum. This charge envelope is then deconvoluted back to the original intact mass through an algorithm in the software that seeks the common numerator, and a reconstructed mass spectrum is generated. For His_6-S6K1αII (ΔAID)-T389E purified from cells solely infected, the reconstructed mass spectrum showed a predominant species *a* (46,558 ± 10 Da) and a very small amount of species *b* (46,638 ± 10 Da) (Fig. 3A). These molecular masses correspond well with the calculated molecular masses of unmodified (46,568 Da) and monophosphorylated His_6-S6K1αII(ΔAID)-T389E [46,648 Da (=46,558 + 80)]. Similarly, this enzyme preparation eluted as a single species *a* in MonoQ anion exchange chromatography (42.2% Buffer B or 0.433 M NaCl) for which negligible catalytic activity was observed (2 ± 1 nmol/min/mg) (Fig. 3B). The hint of a small shoulder is also present in the chromatogram (45.5% Buffer B or 0.466 M NaCl), likely corresponding to the very tiny amount of a monophosphorylated species.

After 30 min in vitro treatment of unphosphorylated His_6-S6K1αII(ΔAID)-T389E with His_6-PDK1(ΔPH), the reconstructed mass spectrum showed about equal amounts of species *a* (46,558 ± 10 Da) and species *b* (46,638 ± 10 Da) (Fig. 3C), which were partially resolved in MonoQ anion exchange chromatography (species *a*: 42.2% Buffer B or 0.433 M NaCl; species *b*: 45.5% Buffer B or 0.466 M NaCl) (Fig. 3D). These results are consistent with the 0.5 mole fraction (Fig. 2D) of site-specific T229 phosphorylation (Fig. 2E). Due to the inability to completely fractionate the unphosphorylated (species *a*) and T229 monohosphorylated isoforms (species *b*), S6K1 activities of ~20 and ~120 nmol/min/mg were recorded for fractions collected for enzyme species *a* and *b*, respectively (Fig. 3D). In addition, a small amount of species *c* (46,718 ± 10 Da) was detected by ESI-TOF (Fig. 3C), which corresponds to the calculated molecular mass of diphosphorylated His_6-S6K1αII(ΔAID)-T389E. Since it was not readily identified in the MonoQ chromatogram (Fig. 3D), the amount was insufficient for determination of its activity. The detection of this small amount of diphosphorylated species *c* is consistent with SDS-PAGE and Western detection of a tiny amount of slower mobility T229 phosphorylated His_6-S6K1αII(ΔAID)-T389E (Fig. 2C, lane 3).

For His_6-S6K1αII(ΔAID)-T389E purified from cells coinfected with His_6-PDK1(ΔPH), the reconstructed mass spectrum showed about equal amounts of species *b* (46,638 ± 10 Da) and species *c* (46,718 ± 10 Da) (Fig. 3E), which were partially resolved in MonoQ anion exchange chromatography (species *b*: 45.5% Buffer B or 0.466 M NaCl; species *c*: 48.5% Buffer B or 0.495 M NaCl) (Fig. 3F). The detection of approximately equal amounts of monophosphorylated species *b* and diphosphorylated species *c* is consistent with SDS-PAGE and Western detection of significant amounts of two distinct T229 phosphorylated His_6-S6K1αII(ΔAID)-T389E species, which migrate with slightly different mobilities (Fig. 2C, lane 2). Importantly, S6K1 enzyme activities of 250 ± 10 nmol/min/mg were determined for both fractionated enzyme species (Fig. 3F), indicating that the second site of phosphorylation renders no effect on S6K1 catalytic activity.

Interestingly, purified His_6-S6K1αII(ΔAID)-T389E displayed anomalously slower mobility in SDS-PAGE ($M_r \approx 50$ kDa versus $M_{calc} = 46{,}568$ Da) (Fig. 2A, lane 3). However, neither phosphorylation nor any other post-translational modification was detected by ESI-TOF analysis of His_6-S6K1αII(ΔAID)-T389E purified from Sf9 cells solely infected. It has been pointed out that due to their unique amino acid compositions, intrinsically disordered peptide regions bind less SDS and therefore may contribute to aberrant slower mobilities in SDS-PAGE

[15]. The significant amount of peptide regions in His_6-S6K1αII(ΔAID)-T389E predicted to be disordered by the PONDR® analysis (Supplementary Material, Fig. S1) likely accounts for the observed slower mobility of His_6-S6K1αII(ΔAID)-T389E in SDS-PAGE.

Steady-state kinetics of PDK1 activated His_6-S6K1αII(ΔAID)-T389E

Steady-state kinetic titrations of (i) in vivo and (ii) in vitro PDK1-activated His_6-S6K1αII (ΔAID)-T389E were carried out with varying concentrations of either S6K1-Tide (Fig. 4A) or ATP (Fig. 4B), while maintaining a saturating concentration of the other substrate. To better highlight the similarities and differences in steady-state kinetic parameters, the Michaelis-Menten equation was rearranged and the data were plotted as linear plots of k versus k/[S] according to Eq. 1:

$$k = -K_m\left(\frac{k}{[S]}\right) + k_{cat} \quad (1)$$

in which the y-intercept, slope, and x-intercept correspond to the apparent values of k_{cat}, K_m, and k_{cat}/K_m, respectively. The parallel nature of the plots determined for the two different methods of S6K1 activation with respect to each given substrate (Fig. 4) show that the observed increased activity of His_6-S6K1αII(ΔAID)-T389E, purified from Sf9 cells coinfected with His_6-PDK1(ΔPH), is manifest entirely in k_{cat}. For titrations with S6K1-Tide (Fig. 4A), apparent values of (i) $k_{cat} = 0.19 \pm 0.01$ s^{-1} and $K_m^{Tide} = 3.6 \pm 0.3$ μM and (ii) $k_{cat} = 0.057 \pm 0.003$ s^{-1} and $K_m^{Tide} = 3.7 \pm 0.4$ μM were obtained for (i) in vivo and (ii) in vitro PDK1-activated His_6-S6K1αII(ΔAID)-T389E, respectively. For titrations with ATP (Fig. 4B), apparent values of (i) $k_{cat} = 0.19 \pm 0.01$ s^{-1} and $K_m^{ATP} = 5.4 \pm 0.4$ μM and (ii) $k_{cat} = 0.057 \pm 0.004$ s^{-1} and $K_m^{ATP} = 4.8 \pm 0.6$ μM were obtained for (i) in vivo and (ii) in vitro PDK1-activated His_6-S6K1αII(ΔAID)-T389E, respectively. It is important to point out that although in vitro activation by PDK1 resulted in 50% T229 phosphorylation, 50% of k_{cat} (125 U/mg or 0.09 s^{-1}) could not be achieved, likely due to partial inactivation of His_6-S6K1αII(ΔAID)-T389E during 30 min treatment with PDK1 at 25 °C.

Summary

Overall, we conclude that the highly active form of His_6-S6K1αII(ΔAID)-T389E, as purified from cells coinfected with His_6-PDK1(ΔPH), is most suitable for biophysical studies of S6K1 substrate binding and chemical catalysis. Initial coinfection of 200 mL of Sf9 insect cells (2×10^6 cells/mL) with MOI = 1 for each recombinant baculovirus and harvesting after 56-60 h yielded approximately equal amounts of His_6-PDK1(ΔPH) (8 ± 2 mg) and His_6-S6K1αII (ΔAID)-T389E (5 ± 1 mg). After His_6 affinity co-purification, which was carried out to verify expression amounts of both constructs, His_6-S6K1αII(ΔAID)-T389E was easily separated from His_6-PDK1(ΔPH) by MonoQ anion exchange chromatography at pH 7.3, whereby His_6-PDK1(ΔPH) was not retained by the column and His_6-S6K1αII(ΔAID)-T389E eluted between 0.46 and 0.50 M NaCl as approximately equal amounts of two equally high active species (250 ± 10 nmol/min/mg). Western analysis and ESI-TOF mass spectrometry confirmed full T229 phosphorylation in both species, as well as one other site of phosphorylation in the second species that did not affect enzyme activity. ESI-TOF detected tiny amounts of higher degree phosphorylated species. The purified ~100% T229 phosphorylated active His_6-S6K1αII(ΔAID)-T389E yielded steady-state kinetic parameter values of $k_{cat} = 0.19 \pm 0.01$ s^{-1}, $K_m^{Tide} = 3.6 \pm 0.3$ μM, and $K_m^{ATP} = 5.4 \pm 0.4$ μM.

Initial single infection of 200 mL of Sf9 insect cells (2×10^6 cells/mL) with MOI = 2 and harvesting after 56-60 h gave high yields of His_6-S6K1αII(ΔAID)-T389E (15 ± 2 mg). His_6 affinity purified His_6-S6K1αII(ΔAID)-T389E eluted predominantly as a single peak near 0.43 M NaCl and was essentially inactive enzyme (2 ± 1 nmol/min/mg). Western analysis and ESI-

TOF mass spectrometry confirmed very little or no T229 phosphorylation. While both Western analysis and ^{32}P-phosphopeptide mapping demonstrated site-specific in vitro T229 phosphorylation by purified His_6-PDK1(ΔPH), under no conditions could mole fraction amounts exceeding ~50% be achieved. As such, in vitro PDK1-activated His_6-S6K1αII (ΔAID)-T389E eluted between 0.43 and 0.46 M NaCl as approximately equal amounts of the unphosphorylated and T229 phosphorylated isoforms, which was confirmed by ESI-TOF mass spectrometry. The purified ~50% T229 phosphorylated His_6-S6K1αII(ΔAID)-T389E yielded steady-state kinetic parameter values of $k_{cat} = 0.057 \pm 0.004\ s^{-1}$, $K_m^{Tide} = 3.7 \pm 0.4\ \mu M$, and $K_m^{ATP} = 4.8 \pm 0.6\ \mu M$. On consolation, the largely homogeneous unmodified His_6-S6K1αII (ΔAID)-T389E, purified from Sf9 cells solely infected, is deemed suitable for biophysical studies of PDK1-catalyzed T229 phosphorylation. Of particular interest will be characterization of the reaction steps that give rise to the noticeable lag kinetics and sub-stoichiometric amount of T229 phosphorylated product. The significant amount of peptide regions in His_6-S6K1αII(ΔAID)-T389E predicted to be disordered by the PONDR® analysis (Supplementary Material), which gives rise to the observed slower mobility of His_6-S6K1αII (ΔAID)-T389E in SDS-PAGE, may serve as points of interest with regard to S6K1 reactivity and stability.

Supplementary Material

Refer to Web version on PubMed Central for supplementary material.

Acknowledgements

This research was supported by a grant from the National Institute of General Medical Sciences (GM69868) to T.K.H. and a Maytag Fellowship to M.M.K. We kindly thank Bob O'Meally and Bob Cole of the Mass Spectrometry/ Proteomics Core Facility at Johns Hopkins University for ESI-TOF mass spectrometry data collection and analysis.

References

1. Holz MK, Ballif BA, Gygi SP, Blenis J. mTOR and S6K1 mediate assembly of the translation preinitiation complex through dynamic protein interchange and ordered phosphorylation events. Cell 2006;123:569–580. [PubMed: 16286006]
2. Tee AR, Blenis J. mTOR, translational control and human disease. Semin. Cell Dev. Biol 2005;16:29–37. [PubMed: 15659337]
3. Fingar DC, Blenis J. Target of rapamycin (TOR): an integrator of nutrient and growth factor signals and coordinator of cell growth and cell cycle progression. Oncogene 2004;23:3151–3171. [PubMed: 15094765]
4. Richardson CJ, Schalm SS, Blenis J. PI3-kinase and TOR: PIKTORing cell growth. Semin. Cell Dev. Biol 2004;15:147–159. [PubMed: 15209374]
5. Martin KA, Blenis J. Coordinate regulation of translation by the PI 3-kinase and mTOR pathways. Adv. Cancer Res 2002;86:1–39. [PubMed: 12374276]
6. Grove JR, Banerjee P, Balasubramanyam A, Coffer PJ, Price DJ, Avruch J, Woodgett JR. Cloning and expression of two human p70 S6 kinase polypeptides differing only at their amino termini. Mol. Cell Biol 1991;11:5541–5550. [PubMed: 1922062]
7. Peterson RT, Schreiber SL. Kinase phosphorylation: keeping it all in the family. Curr. Biol 1999;9:R521–R524. [PubMed: 10421571]
8. Alessi D, Kozlowski MT, Weng Q-P, Morrice N, Avruch J. 3-Phosphoinositide-dependent protein kinase 1 (PDK1) phosphorylates and activates the p70 S6 kinase in vivo and in vitro. Curr. Biol 1997;8:69–81. [PubMed: 9427642]
9. Pullen N, Dennis PB, Andjelkovic M, Dufner A, Kozma SC, Hemmings BA, Thomas G. Phosphorylation and activation of $p70^{s6k}$ by PDK1. Science 1998;279:707–710. [PubMed: 9445476]
10. Frödin M, Antal TL, Dümmler BA, Jensen CJ, Deak M, Gammeltoft S, Biondi RM. A phosphoserine/threonine-binding pocket in AGC kinases and PDK1 mediates activation by hydrophobic motif phosphorylation. EMBO J 2002;21:5396–5407. [PubMed: 12374740]

11. Balendran A, Currie R, Armstrong CG, Avruch J, Alessi DR. Evidence that 3-phosphoinositide-dependent protein kinase-1 mediates phosphorylation of p70 S6 kinase in vivo at Thr-412 as well as Thr-252. J. Biol. Chem 1999;274:37400–37406. [PubMed: 10601311]

12. Biondi RM, Kieloch A, Currie RA, Deak M, Alessi DR. The PIF-binding pocket in PDK1 is essential for activation of S6K and SGK, but not PKB. EMBO J 2001;20:4380–4390. [PubMed: 11500365]

13. Zhang W-G, Shor B, Yu K. Identification and characterization of a constitutively T-loop phosphorylated and active recombinant S6K1: expression, purification, and enzymatic studies in a high capacity non-radioactive TR-FRET Lance assay. Prot. Express. Purif 2006;46:414–420.

14. Neet KE, Ainslie GR. Hysteretic enzymes. Methods Enzymol 1980;64:192–226. [PubMed: 7374453]

15. Receveur-Bréchot V, Bourhis J-M, Uversky VN, Canard B, Longhi S. Assessing protein disorder and induced folding. Proteins: Struct. Funct. Genet 2006;62:24–45. [PubMed: 16287116]

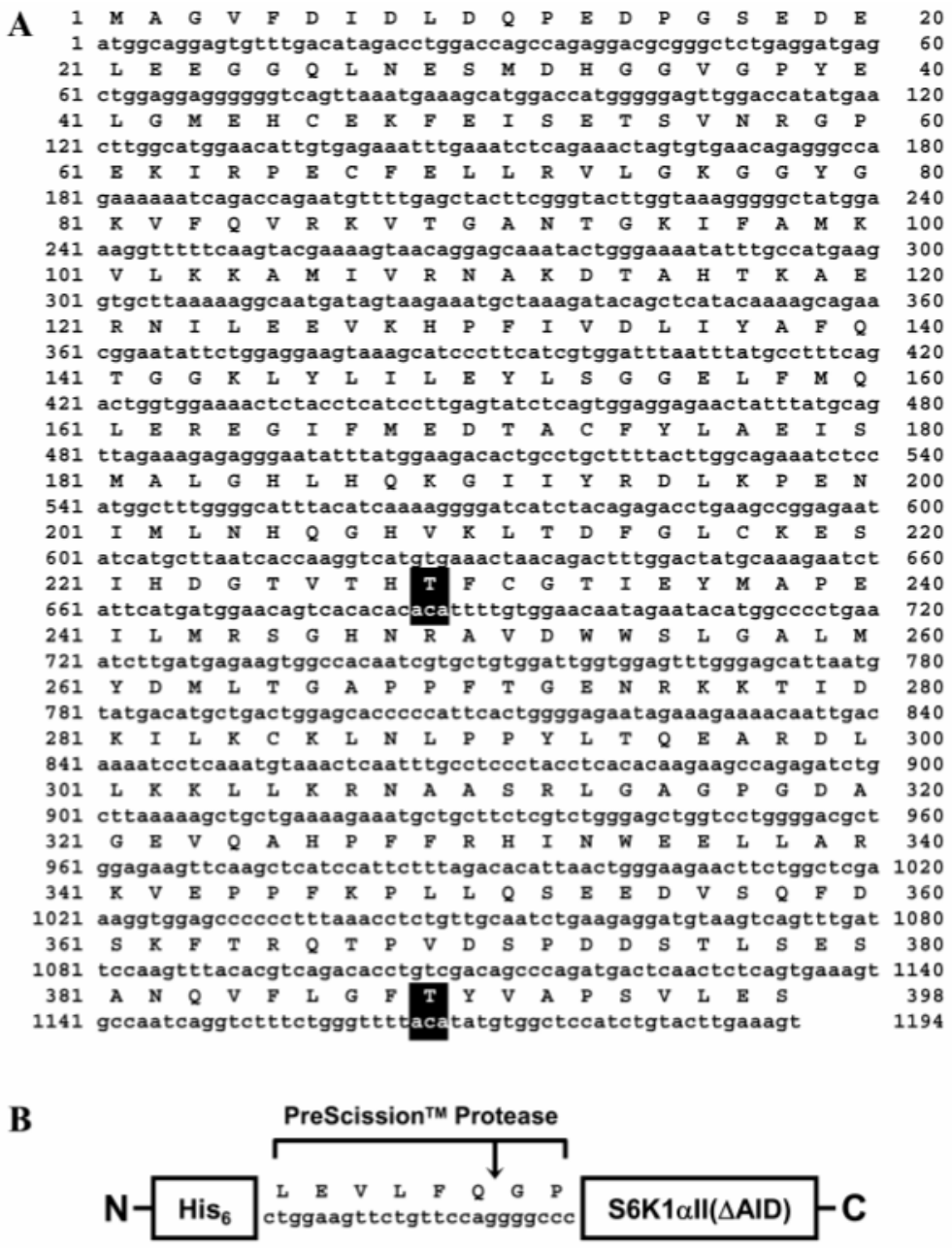

Fig. 1.

S6K1 expression construct. (A) Amino acid and DNA coding sequence of the N-terminal catalytic kinase domain of the 70 kDa 40S ribosomal protein S6 kinase-1 [S6K1(ΔAID); residues 1-398 in the S6K1αII isoform). The regulatory sites of T-loop (T229) and hydrophobic motif phosphorylation (T389) are shaded. (B) S6K1(ΔAID) was engineered in the pFastbac™1 vector to contain and N-terminal His_6 affinity tag, the PreScission protease recognition sequence, and the T389E phosphomimicking mutation.

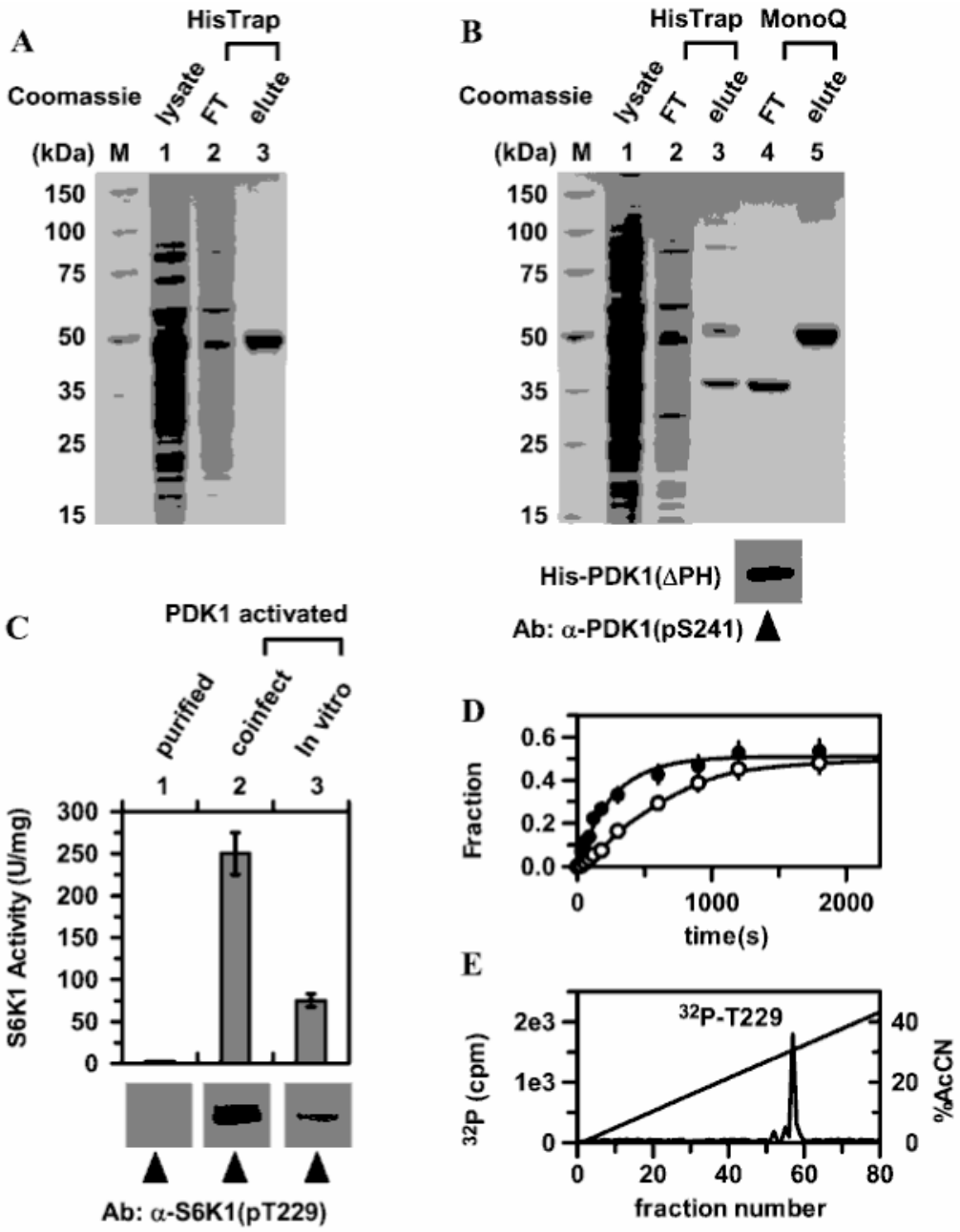

Fig. 2.

Expression, purification, and activation of His_6-S6K1αII(ΔAID)-T389E by PDK1. (A) SDS-PAGE analysis with Coomassie staining of His_6-S6K1αII(ΔAID)-T389E purified after baculovirus-mediated expression and His_6 affinity purification from Sf9 insect cells. Lane 1 shows the total soluble lysate; lane 2 shows the proteins from the soluble lysate that were not retained after passage over the His_6 affinity column; and lane 3 shows purified His_6-S6K1αII (ΔAID)-T389E subsequently eluted from the His_6 affinity column. (B) SDS-PAGE analysis with Coomassie staining of His_6-S6K1αII(ΔAID)-T389E purified from Sf9 insect cells that were coinfected with His_6-PDK1(ΔPH). Lane 1 shows the total soluble lysate; lane 2 shows the proteins from the soluble lysate that were not retained after passage over the His_6 affinity column; lane 3 shows both His_6-S6K1αII(ΔAID)-T389E and His_6-PDK1(ΔPH), which co-

eluted from the His_6 affinity column; lane 4 shows purified His_6-PDK1(ΔPH) that was not retained by the MonoQ anion exchange column and shown below is Western detection of S241 phosphorylated His_6-PDK1(ΔPH) using the phospho-PDK1 (S241) polyclonal antibody; and lane 5 shows His_6-S6K1αII(ΔAID)-T389E that eluted from the MonoQ anion exchange column. (C) Comparison of His_6-S6K1αII(ΔAID)-T389E activation by (i) S6K1 activity towards the model S6K1-Tide and (ii) SDS-PAGE-Western analysis using the phospho-S6K1 (T229) polyclonal antibody. Lane 1 shows His_6-S6K1αII(ΔAID)-T389E purified from cells solely infected; lane 2 shows His_6-S6K1αII(ΔAID)-T389E purified from cells coinfected with His_6-PDK1(ΔPH); and lane 3 shows His_6-S6K1αII(ΔAID)-T389E purified from cells solely infected after 30 min in vitro treatment with His_6-PDK1(ΔPH). (D) Progress curves for PDK1-catalyzed phosphorylation of His_6-S6K1αII(ΔAID)-T389E. Either 2 μM (●) or 15 μM (○) His_6-S6K1αII(ΔAID)-T389E was incubated at 25 °C with 10 nM active His_6-PDK1(ΔPH) and 100 μM [γ-^{32}P]ATP in kinase reaction buffer. At different times, aliquots were removed from the reaction mixture, and the mole fraction of phosphorylated His_6-S6K1αII(ΔAID)-T389E was determined. (E) After 30 min treatment of His_6-S6K1αII(ΔAID)-T389E with His_6-PDK1 (ΔPH) and [γ-^{32}P]ATP-Mg^{2+}, the reaction mixture was subjected to proteolytic digestion with trypsin and the resulting peptides were resolved by reversed-phase HPLC. Scintillation counting of the individual fractions detected the ^{32}P-radiolabeled peptide that eluted near 31% acetonitrile, which has been identified by Edmond degradation to be the monophosphorylated tryptic peptide containing ^{32}P-T229 [8].

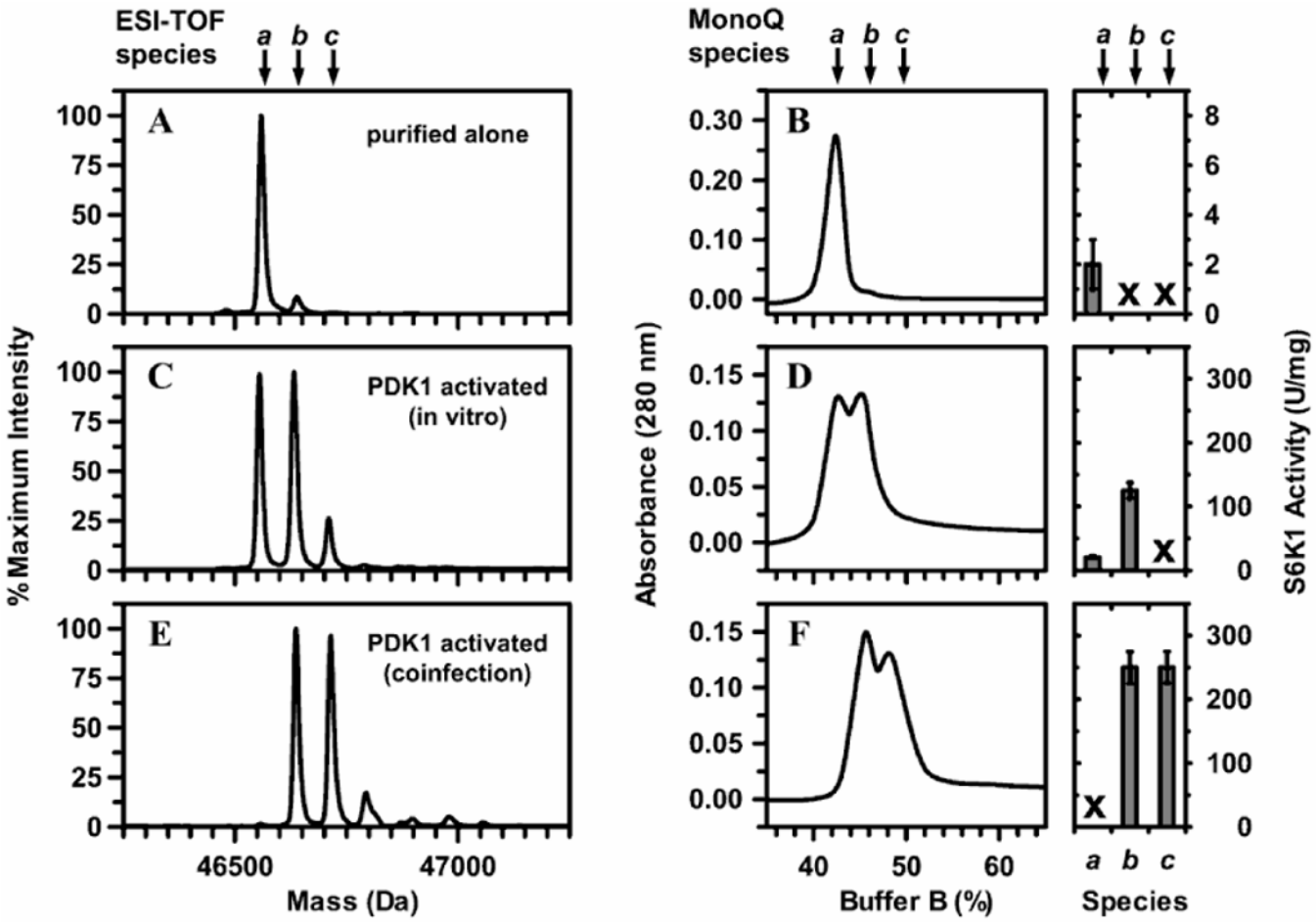

Fig. 3.

ESI-TOF and MonoQ analysis of His_6-S6K1αII(ΔAID)-T389E phospho-isoform species. (A, C, E) ESI-TOF reconstructed mass spectra and (B, D, F) MonoQ elution profiles and the corresponding S6K1 activities measured for fractionated phospho-isoform species are shown for (A, B) His_6-S6K1αII(ΔAID)-T389E purified from cells solely infected; (C, D) His_6-S6K1αII(ΔAID)-T389E purified from cells solely infected after 30 min in vitro treatment with His_6-PDK1(ΔPH); and (E, F) His_6-S6K1αII(ΔAID)-T389E purified from cells coinfected with His_6-PDK1(ΔPH). For each reconstructed mass spectrum, species *a* (46,558 ± 10 Da), *b* (46,638 ± 10 Da), and *c* (46,714 ± 10 Da) correspond to the calculated molecular masses of the unmodified (46,568 Da), monophosphorylated (46,648 Da), and diphosphorylated forms of His_6-S6K1αII(ΔAID)-T389E (46,728 Da). For His_6-S6K1αII(ΔAID)-T389E purified from cells coinfected with His_6-PDK1(ΔPH), ESI-TOF detected a small amount of triphosphorylated enzyme and very small amounts of even higher order phosphorylated species. The MonoQ elution peaks of species *a*, *b*, and *c* were maximum at 42.4%, 45.5%, and 48.5% of Buffer B; and the fractions corresponding to the peak maximums were assayed for S6K1 activity towards the model S6K1-Tide. In cases where no significant amount of enzyme eluted as a designated species, activities could not be determined and are so denoted (×).

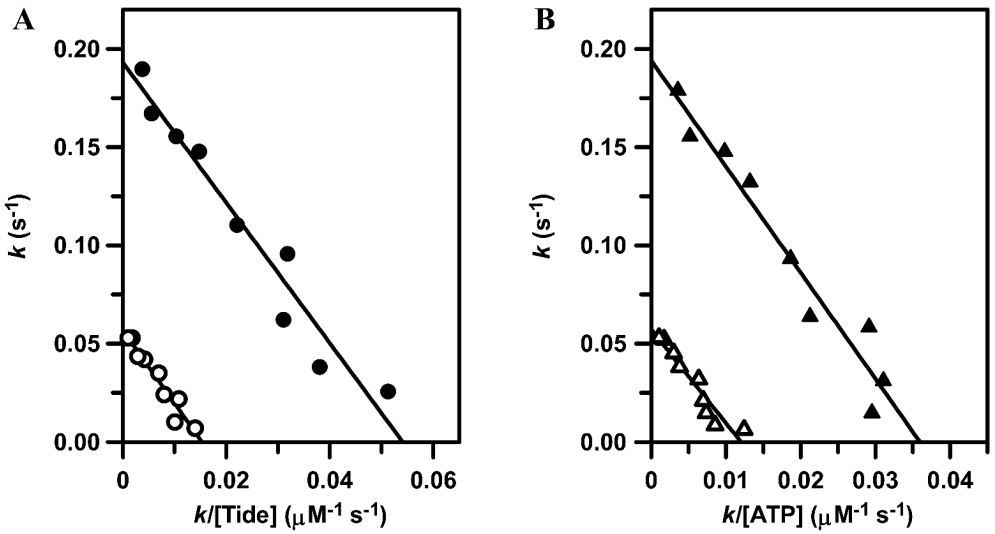

Fig. 4.

Steady-state kinetic titrations of His_6-S6K1αII(ΔAID)-T389E with nucleotide and peptide substrates. (A) Titration of in vivo (●) and in vitro (○) PDK1-activated His_6-S6K1αII(ΔAID)-T389E with varying S6K1-Tide concentrations. (B) Titration of in vivo (▲) and in vitro (△) PDK1-activated His_6-S6K1αII(ΔAID)-T389E with varying S6K1-Tide concentrations. Initial velocities normalized to enzyme concentration ($k = v/[E_t]$) were measured (A) using 50 μM ATP for varying S6K1-Tide concentrations (0.5, 1, 2, 3, 5, 10, 15, 30, and 50 μM) and (B) using 50 μM S6K1-Tide for varying ATP concentrations (0.5, 1, 2, 3, 5, 10, 15, 30, and 50 μM). The assays were initiated by addition of 20 nM kinase.

Table 1

Purification of His_6-S6K1αII(ΔAID)-T389E from Sf9 cells solely infected[a]

Purification (Step)	Volume (mL)	Concentration (mg/mL)	Yield (mg)	Purification (fold)
Crude lysate	50	3.6 ± 0.2	180 ± 10	N/A
Ni Sepharose	15	1.1 ± 0.1	15 ± 2	12

[a] All values are reported for purification from initial infection of 200 mL of insect Sf9 cells (2×10^6 cells/mL) with recombinant baculovirus.

Table 2

Purification of His_6-S6K1αII(ΔAID)-T389E from Sf9 cells coinfected with His_6-PDK1(ΔPH)[a]

Purification (Step)	Volume (mL)	Concentration (mg/mL)	Yield (mg)	Purification (fold)
Crude lysate	50	3.6 ± 0.2	180 ± 10	N/A
Ni Sepharose	15	1.0 ± 0.1	15 ± 1.6	12
MonoQ	12	0.43 ± 0.07	5 ± 1	36

[a] All values are reported for purification from initial infection of 200 mL of insect Sf9 cells (2×10^6 cells/mL) with recombinant baculovirus.